Influence of Cd impurity on the electronic properties of $CuAlO_2$ delafossite: first-principles calculations

Influence of Cd impurity on the electronic properties of CuAlO₂ delafossite: first-principles calculations

M V Lalić[1]**, J Mestnik-Filho, A W Carbonari, R N Saxena and M Moralles**

Instituto de Pesquisas Energéticas e Nucleares, PO Box 11049, 05422-970 São Paulo, SP, Brazil

E-mail: jmestnik@net.ipen.br

Abstract

We report on first-principles band-structure calculations of the semiconducting CuAlO₂ delafossite compound in the pure form and also with Cd impurity occupying either a Cu or Al position. The computational tool was a full-potential linear augmented plane-wave method, with the generalized gradient approximation accounting for the exchange and correlation effects. The changes caused by the presence of Cd are studied by the analysis of the electronic structure and the electric field gradient (EFG) in both Cd-doped and pure CuAlO₂ systems. Good agreement between the calculated and measured EFGs at Cd substituting for Cu or Al atoms in CuAlO₂ indicates that the calculations were able to correctly describe the ground state of the system containing the impurity. It is shown that a specific hybridization scheme, involving Cu (and Cd) s and d_{z^2} orbitals and neighbouring O p_z orbitals, takes place at the Cu sites in CuAlO₂ as proposed earlier. The results of the calculations indicate that the Cd-doped system changes its electrical properties when Cd replaces Cu atoms (producing an n-type semiconductor), but not when it substitutes for Al atoms.

1. Introduction

The delafossite-type compounds have a chemical formula ABO₂, where A is a monovalent metal ion (Cu, Ag, Pd, Pt) and B is a trivalent ion (Al, In, Cr, Co, Fe etc). Their electrical properties depend on which ion occupies the A site: Pd and Pt (d^9 ions) result in conductivity, while Cu and Ag (d^{10} ions) produce semiconductivity [1]. The crystal structure, shown in figure 1, can be viewed as an alternative stacking of the A and BO₂ layers perpendicular to the *c*-axis. Each A atom is linearly coordinated by two oxygens along the *c*-axis, and has another six A atoms in the basal plane as second neighbours. The B atom is octahedrally surrounded by six oxygens, while each O is coordinated tetrahedrally by one A and three B atoms.

---

[1] On leave from: Institute of Nuclear Sciences 'Vinča', PO Box 522, 11001 Belgrade, Yugoslavia.
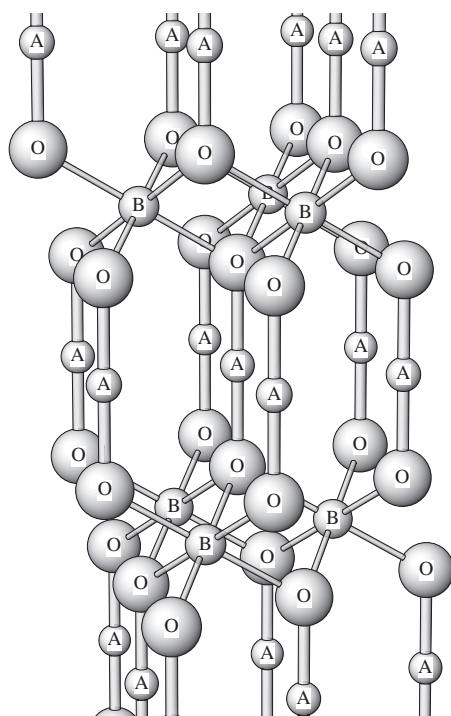
Figure 1. The ABO$_2$ delafossite crystal structure.

Several features of delafossites, e.g. the linear coordination of the A atom and the anisotropy of the electrical conductivity, have been qualitatively explained in terms of a simple model of chemical bonding occurring at the A site, as suggested by Rogers *et al* [1]. The model is based on the previous observation of Orgel [2] that linear coordination of the d^{10} ion can be stabilized by a non-spherical electron configuration if the energy separation between s and d orbitals is sufficiently small. In that case, s and d$_{z^2}$ orbitals hybridize, forming a filled bonding $(1/\sqrt{2})(s - d_{z^2})$ and an empty antibonding $(1/\sqrt{2})(s + d_{z^2})$ orbital (the *z*-axis is taken to be parallel to the *c*-axis of the crystal, throughout the paper). The bonding orbital has charges concentrated mainly in the basal plane, which significantly lowers the energy of the A ion in linear coordination, and gives rise to larger conductivity in the basal plane due to electron hopping between neighbouring A-ion orbitals. On the other hand, the antibonding orbital is used for mixing with neighbouring O sp^3 orbitals, making a bonding complex that lies deep below the Fermi energy and an antibonding complex that forms a conduction band. Recently, semiconducting delafossite oxides have attracted much attention due to their promise for technological applications. Having large band gaps, these materials are optically transparent and can be used as optoelectronic devices. Previously known semiconducting transparent oxides, such as doped versions of In$_2$O$_3$, SnO$_2$ and ZnO, show only n-type conductivity and therefore their application has been limited to transparent electrodes [3]. It has been shown, however, that the delafossites can be made both n- and p-type semiconductors [4–7], which opened the possibility of constructing a delafossite p–n junction which will transmit visible light and at the same time generate electricity by absorption of ultraviolet photons (transparent transistor). Despite the fact that a delafossite compound with necessary high p-type conductivity has not yet been found, the subject is still the focus of interest.

The progress in the theoretical understanding of the electronic properties of delafossites has been much slower than the experimental progress. Only recently have first-principles band-structure calculations of the pure CuAlO$_2$ become available [8, 9]. However, theoretical calculations are lacking for delafossites containing impurities that could provide a deeper understanding of their semiconducting properties.

In this paper we report on first-principles electronic structure calculations of CuAlO$_2$ delafossite in the pure form and with a Cd impurity substituting at either Cu or Al positions. Our goal is twofold:

(1) to investigate the changes of the electronic structure caused by the presence of an impurity; and
(2) to check the validity of the s–d hybridization scheme at the Cu site in this compound.

During the course of our work we became aware of another article reporting on full-potential linear augmented plane-wave (FPLAPW) calculations for pure CuAlO$_2$ [10] in which the s–d hybridization scheme for Cu is also discussed. However, the analysis presented here contains more details and is carried out not just for Cu, but also for Cd substituting at the Cu site. Cadmium was chosen as an impurity for the present calculations since experimental measurements of the electric field gradient (EFG) at Cd nuclei occupying both Cu and Al sites in CuAlO$_2$ are already available from perturbed angular correlation (PAC) experiments [11, 12]. As the EFG is a quantity that depends sensitively on the details of the electronic structure [13, 14], a comparison of the calculated values with experimentally measured EFGs can be used to test the validity of our theoretical results.

CuAlO$_2$ was the first delafossite reported to exhibit p-type conductivity, even without any intentional doping [4]. This property has been attributed to the presence of natural defects that induce excess of oxygen (a Cu site vacancy or an interstitial O). Results of the present study indicate that CuAlO$_2$ can exhibit n-type conductivity also, if the system is doped with Cd atoms substituting at Cu sites. Thus, the CuAlO$_2$ shows bipolarity in electrical conduction, and a p–n junction can in principle be constructed from this compound alone.

2. Calculation details

The crystal structure of CuAlO$_2$ belongs to the space group $R\bar{3}m$. The primitive unit cell is rhombohedral and contains four atoms. The Cu occupies the 1a site, Al the 1b site, and the O 2c sites, according to Wyckoff's notation. While the Cu and Al positions are fixed by symmetry, the O position is determined by the internal parameter u. We have used the experimental value of $u = 0.109\,79$, taken from [15]. Values for the lattice parameters are taken from [16] and they refer to a hexagonal description of the unit cell ($a = 2.857$ Å, $c = 16.940$ Å). The corresponding rhombohedral lattice parameters are: $a_r = 5.883$ Å and $\alpha = 28.1075°$.

The presence of Cd impurities in CuAlO$_2$ is simulated in calculations by using a supercell approach. The supercell is constructed by doubling the rhombohedral lattice parameter a_r of the pure CuAlO$_2$ unit cell. It thus consists of 8 original unit cells, containing 32 atoms inside. The Cd atom is then placed at the position of one of the Cu atoms forming the first supercell. The second supercell is formed similarly by placing the Cd atom at an Al position.

Self-consistent band-structure calculations for pure CuAlO$_2$ as well as for the compound containing Cd at the Cu and Al positions were performed using the WIEN97 computer code [17], which is based on the application of the FPLAPW method [18]. In this method, the electronic wavefunctions, charge density and crystal potential are expanded in spherical harmonics inside the non-overlapping spheres centred at each nuclear position (with radii R_{MT}), and in plane waves in the rest of the space (interstitial region). For the atomic sphere
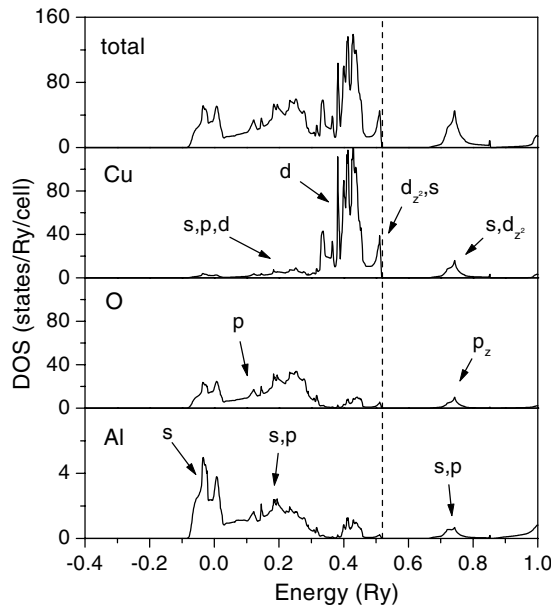
Figure 2. The FPLAPW DOS and PDOS of the CuAlO$_2$ compound. Predominant orbital characters of bands are indicated. The dashed line denotes the Fermi level.

radii R_{MT}, we have chosen a value of 1.9 au for Cu, Al and Cd, and 1.5 au for oxygen, in all three cases. Inside the atomic spheres, the partial waves were expanded up to $l_{max} = 6$, while the number of plane waves in the interstitial was limited by the cut-off at $K_{max} = 8.0/R_{MT}$ for pure compounds, and at $K_{max} = 7.0/R_{MT}$ for compounds containing Cd. The number of plane-wave basis functions in the interstitial region was 1823 for the pure and 9088 for the impurity-containing systems. The charge density was Fourier expanded up to $G_{max} = 14$. For a Brillouin zone integration, a mesh of 110 $\vec{k}$-points in the irreducible part of the zone was used in the case of pure CuAlO$_2$ and 28 $\vec{k}$-points in cases where Cd was present. Exchange and correlation effects were treated within density functional theory with the generalized gradient approximation (GGA96) [19]. The following atomic states: Cu: $3p^63d^{10}4s^1$, Al: $2p^63s^23p^1$, O: $2s^22p^4$ and Cd: $4p^64d^{10}5s^2$ were considered as valence states, in all three calculated structures. In the process of solving the radial equations these states were treated within the scalar-relativistic approach, whereas the core states were treated in a fully relativistic manner. Inside the supercells containing Cd the optimization of all atomic positions has been performed using the force minimization method, while the lattice parameters were kept fixed. More details about the computational parameters mentioned above, as well as about criteria for their choice, can be found in [17].

3. Electronic structure

3.1. Pure CuAlO$_2$

The FPLAPW density of states (DOS) of the pure CuAlO$_2$ compound, as well as the projected density of states (PDOS) for each inequivalent atom, are presented in figure 2. A semiconducting solution has been obtained with a fundamental gap of 1.97 eV, in agreement with the FPLAPW value of 1.95 eV reported by Ingram *et al* [10]. A smaller value of 1.7 eV

was calculated by Yanagi *et al* [9] who used a FPLAPW method as well. The origin of this discrepancy is difficult to trace since the parameters used in [9] were not reported. From photo-electrochemical measurements the indirect band gap in CuAlO$_2$ is found to be 1.65 eV [20], while an estimation from an optical transmission spectrum gave a value of ∼1.8 eV [9].

The valence band consists mostly of O 2p and Cu 3d states, and the same is true for the first peak in the conduction band DOS. The Al states contribute very little to the valence DOS, and do not play an electrically active role in the compound. The O orbitals are not in sp^3 hybridized states, as assumed in the s–d hybridization model [1], since O s and p states are well separated in energy (s states are positioned around −0.9 Ryd). Instead, it is the O p$_z$ orbital that makes the bonds with neighbouring Cu orbitals. Except for this detail, a careful analysis of the CuAlO$_2$ electronic structure confirms the validity of s–d hybridization scheme. The peak positioned at the Fermi level consists of Cu s and d$_{z^2}$ states, with a negligible contribution from O p$_z$ states. This peak can be identified as originating from a bonding $(1/\sqrt{2})(s - d_{z^2})$ orbital of Cu, in which the charge is concentrated mostly in the basal plane with lobes pointing towards the neighbouring copper atoms. The first peak at the conduction band resulted mostly from Cu s, d$_{z^2}$ and O p$_z$ states and therefore corresponds to the antibonding combination of the Cu $(1/\sqrt{2})(s + d_{z^2})$ orbital and the O p$_z$ orbital. The bonding combination of the same orbitals is positioned in the lower-energy part of the valence band, being considerably broadened due to strong coupling with the other orbitals at the same energies.

3.2. CuAlO$_2$ with Cd impurity substituting for Cu

Replacement of a Cu atom by a Cd impurity causes significant changes in the electronic structure of CuAlO$_2$ as well as in the rearrangement of the atoms around the impurity. To account for the latter, a relaxation of all the atomic positions in the supercell has been performed, going from the non-optimized structure with the same inter-atomic distances as in the pure compound to the optimized structure where the atomic positions are relaxed so that forces acting on each atom are nearly zero. The largest change occurred in the immediate vicinity of Cd in which the two nearest-neighbour (NN) oxygens were pushed away considerably along the crystalline c-axis, changing the Cd–O bond distance from 1.860 to 2.073 Å. As a consequence, the tetrahedral coordination around these oxygen atoms was disturbed in such a way that three Al atoms instead of Cd appeared as their first neighbours. This rearrangement also disturbed the octahedral environments around the Al sites. The Cu atoms in the basal plane were, however, not allowed to move since their lattice positions had been fixed by symmetry.

The changes in the electronic structure are found to be more localized, affecting just the atoms in the closest vicinity of Cd. This fact has been established by monitoring the PDOS and EFG for each inequivalent atom in the supercell, and comparing them with the PDOS and EFG calculated for the same atoms in the pure compound. It has been concluded that significant differences in the electronic structure arise mostly from Cd and its two NN oxygen atoms, as well as (although to a much lesser extent) from the six second-NN copper atoms in the basal plane. Their PDOS, together with the DOS of the compounds with both optimized and non-optimized internal geometries, are presented in figure 3.

When Cd replaces the Cu atom in CuAlO$_2$, it behaves as a donor. The Cd atom donates one extra electron to the valence band and moves the Fermi level into the conduction band (figure 3(a)), leading to a metallic behaviour for the non-optimized structure. Since the Cd d states lie deeper in energy and do not overlap with the broad Cu and O bands, the validity of the s–d hybridization scheme can be more easily verified than in the pure compound. While the Cd bonding $(1/\sqrt{2})(s - d_{z^2})$ orbital cannot be recognized as it is smeared over the wide energy interval from ∼0 to ∼0.5 Ryd, the Cd antibonding $(1/\sqrt{2})(s+d_{z^2})$ orbital is clearly seen
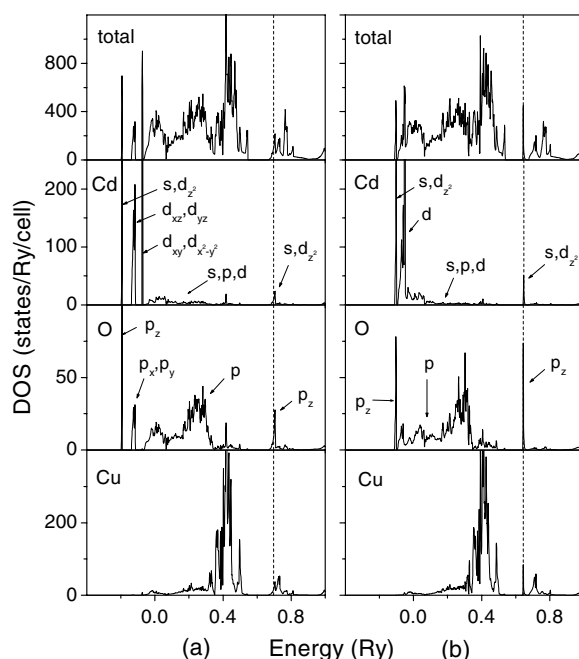
Figure 3. The FPLAPW DOS of Cd-doped CuAlO$_2$ compound, in which Cd substitutes for a Cu atom. The PDOS of Cd, its first-NN O and second-NN Cu are also presented, in both non-optimized (a) and optimized (b) internal geometries. The dashed line denotes the Fermi level.

hybridizing with the O p$_z$ orbital. Their bonding combination can be recognized as a sharp resonance at the energy of $\sim$−0.2 Ryd. The antibonding combination is located at the Fermi level. It constitutes the lower part of the conduction band, together with the Cu s and d orbitals with lobes along the *c*-axis and the Cu–Cd direction (these are d$_{x'^2-y'^2}$ and d$_{z'^2}$ in the local coordinate system in which *x'* is directed along the *c*-axis and *z'* along the Cd–Cu direction). The rest of the atoms in the supercell, more distant from the Cd, have their conduction states not so close to the Fermi level, but a little higher, at energies around 0.75–0.80 Ryd. They constitute the upper part of the conduction band. The difference originates from the fact that Cd, being a donor, introduces a potential which is attractive for the host electrons, and brings the conduction states of the nearest neighbours down in energy.

Optimization of the atomic positions significantly alters the electronic structure of CuAlO$_2$ containing Cd (figure 3(b)). An increase in the Cd–O bond distance stabilizes the orbitals hybridized from Cd $(1/\sqrt{2})(s+d_{z^2})$ and O p$_z$ states, diminishing the energy difference between their bonding and antibonding complexes. As a consequence, the bonding state moves towards higher energies and becomes broad. The antibonding state separates from the rest of the conduction band and goes down inside the energy gap. It forms a band, mainly with the Cu states at the same energies. It is half-filled (contains one electron), and has a non-zero dispersion ($\sim$0.30 eV) due to the finite size of the supercell used in the calculations, in which one cannot completely rule out the possibility of Cd–Cd interactions. The spatial characters of bonding and antibonding complexes are presented in figure 4, showing the respective valence charge densities. While the bonding orbital is localized on Cd and its NN oxygens (figure 4(a)), the antibonding orbital is quite delocalized due to mixing with the Cu states, although a large part of its amplitude is basically centred on Cd, NN oxygens and second-NN copper atoms
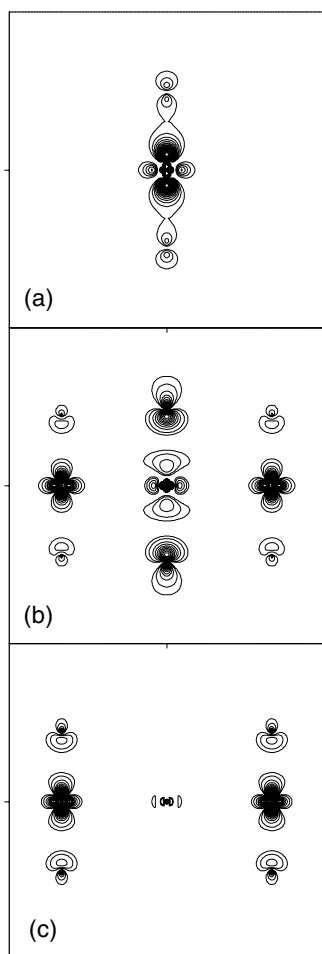
Figure 4. The squared wavefunction of (a) the bonding combination of Cd $(1/\sqrt{2})(s + d_{z^2})$ and O p$_z$ orbitals, (b) the antibonding combination of the same orbitals (mixed with orbitals of neighbouring atoms) that has the energy within the band gap, (c) the conduction band bottom. The projection is onto the XZ-plane, in the Cd-doped CuAlO$_2$ compound, with Cd substituting for a Cu. The Cd nucleus is positioned at the centre of the pictures, with two neighbouring Cu (left and right) along the abscissa. Their neighbouring oxygens are positioned up and down along the ordinate.

(figure 4(b)). While the charge density localized on Cd and O disappeared almost completely, the Cu states remained with the same character as in the conduction band bottom (figure 4(c)).

The present results show that the replacement of Cu by Cd changes the electrical properties of CuAlO$_2$ in a fundamental way. The presence of states inside the gap near the conduction band bottom makes the compound an n-type semiconductor. The fundamental gap (1.90 eV) is somewhat smaller than in the pure compound, and the top of the peak inside the gap is positioned 0.12 eV below the conduction band bottom.

3.3. CuAlO$_2$ with Cd impurity substituting an Al

Introduction of Cd at the Al site in CuAlO$_2$ produces a rearrangement of the host atoms positioned around Cd. The effect is especially large for the six NN oxygen atoms which
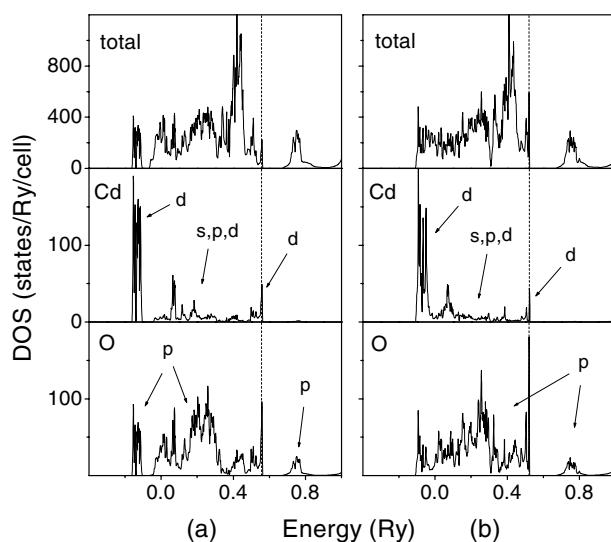
Figure 5. The FPLAPW DOS of Cd-doped CuAlO$_2$ compound, in which Cd replaces an Al atom. The PDOS of Cd and its first-NN O is also presented, in both non-optimized (a) and optimized (b) internal geometries. The dashed line denotes the Fermi level.

octahedrally surround the Cd (see figure 1). As a result of optimization of the atomic positions inside the supercell, they are pushed away from Cd, changing the Cd–O bond distance from 1.910 to 2.106 Å. This movement disturbs the position of the other atoms also, although not very severely.

Most changes of the electronic structure, with respect to the pure compound, originate from the cluster containing Cd and its six NN oxygens. Their PDOS and the DOS of the compound, for both non-optimized and optimized internal geometries, are shown in figure 5. Relatively large changes in the PDOS, and especially in the EFG (where even the sign is reversed), are found at the second-NN Al sites, due to their distorted octahedral environments. However, since Al atoms have very small PDOS in the vicinity of the Fermi level, their contribution to the electrical properties of the compound can be neglected.

Analysis of the DOS shown in figure 5 reveals a different physical picture from the case where Cd substitutes at a Cu site. As the formal valences of Al and Cd ions are respectively +3 and +2, Cd behaves as an acceptor, removing an electron from the valence band. Its perturbing potential is repulsive and thus raises the energy of the valence states of its neighbours. For example, Cd at an Al site gives a Fermi energy of $E_f = 0.557$ Ryd for the non-optimized structure while for the pure compound $E_f = 0.520$ Ryd. A proportion of the Cd d states hybridize with some of the O p states, making a bonding complex, which can be recognized as a resonance around -0.1 Ryd, and an antibonding complex, which is located near the Fermi level (figure 5(a)). Both complexes are mixtures of many orbitals. While the bonding hybrid primarily consists of Cd orbitals with lobes in the basal plane, the antibonding hybrid mostly has Cd orbitals with lobes pointing towards the ligands. Optimization of the atomic positions increases the Cd–O bond length, and diminishes the energy difference between bonding and antibonding complexes (figure 5(b)). The bonding complex moves towards higher energies, joining the rest of the valence band. The antibonding complex moves in the opposite direction, dragging the Fermi level back to the energy of $E_f = 0.521$ Ryd, almost like in the pure compound. It should be noted that the numerical values for Fermi energies do not have any

Table 1. Comparison of the experimental [12] and the theoretical V_{zz}-values in Cd-doped CuAlO$_2$ compounds. V_{zz} is the main component of the EFG tensor, directed along the c-axis of the crystal. The signs of the experimental V_{zz} have not been determined. The data for the Cu and Al are calculated for a pure CuAlO$_2$ compound. The part of the EFG calculated inside the corresponding atomic sphere, originating from valence electrons, is denoted as 'valence V_{zz}'. It is further decomposed into the contributions from p and d electronic shells. A minor s–d contribution, which was not considered important, is not presented. All the numbers given in the table are in units 10^{21} V m^{-2}.

	Experiment $|V_{zz}|$	Theory V_{zz}	Valence V_{zz}		
			p–p contribution	d–d contribution	Total
Cu	—	−5.37	−15.95	10.37	−5.55
Al	—	1.09	1.10	0.03	1.22
Cd at Cu	27.74	−25.74	−20.11	−5.87	−25.73
Cd at Al	7.47	5.63	6.14	−0.29	5.72

physical relevance since they are referred to an unphysical zero. They are presented here in order to illustrate a migration of the valence band top under the impurity influence and effects of the NN relaxation.

Unlike the case in which Cd substitutes for Cu, no states inside the band gap are seen. The perturbing potential of Cd at the Al site is not strong enough to pull the impurity states out from the top of the valence band. The band gap of 2.00 eV is not very different compared to the gap in the pure CuAlO$_2$. Therefore, the electrical properties of the system do not change, and the Cd-doped compound, with Cd substituting for Al, is not a p-type semiconductor.

4. Discussion

The present FPLAPW calculations provide an adequate ground-state description of pure CuAlO$_2$. Since this compound does not represent a strongly correlated electronic system, GGA is a sufficiently good approximation to account for exchange and correlation effects. The underestimation of the fundamental gap is usually expected, but in the present case this quantity is found to be in fair agreement with the experimental value. Reliability of the results obtained for Cd-doped compounds may however be questioned due to the facts that:

(1) the lattice constants were kept fixed during the calculations; and
(2) the size of the supercell was not large enough to avoid Cd–Cd interactions.

To perform calculations that account for these factors, however, would have required much more powerful computational resources than are at present at our disposal. We will therefore try to show in the following that despite these limitations the present calculations can be considered to be sufficiently reliable.

While a systematic relaxation of the lattice parameters was not performed, we made a rough check of the sensitivity of the results by performing additional calculations on two Cd-containing supercells whose volumes were increased by 0.5 and 1.0%. Although the calculated total energies decreased (within the second decimal place in Ryd units), no qualitative changes in the DOS and the EFG were observed. If in fact the Cd–Cd interaction cannot be considered to be negligible in the present calculations due to the rather small supercell, then the results would not be valid for representing an isolated Cd impurity. However, the fact that good agreement was obtained between the calculated and experimental EFGs at Cd substituting both at the Cu sites as well as at the Al sites in CuAlO$_2$ (table 1) suggests that the Cd–Cd interaction does not cause significant changes in the electronic environment of the Cd atoms with respect to the

isolated impurity case. We therefore conclude that the validity of the present calculations can be extended to cases of much lower Cd concentration. The reasoning is based on perceiving that EFG, being a second spatial derivative of the electrostatic potential at the nuclear position, is very sensitive to details of the electronic structure, combined with the fact that the EFG data were experimentally determined for isolated Cd impurity through PAC measurements [11,12]. In these experiments, carrier-free radioactive parent nuclei, ^{111}Ag or ^{111}In (with extremely small ≪0.1 at.% concentrations), were introduced in the CuAlO$_2$ sample by thermal diffusion, occupying Cu or Al atom sites. Following radioactive transformation, both ^{111}Ag and ^{111}In finally decay to the daughter probe nuclei ^{111}Cd where the EFG is measured using the PAC method.

A detailed analysis of the electronic structure in the pure and Cd-doped CuAlO$_2$ compounds has confirmed the validity of the s–d hybridization scheme at the Cu site. The same conclusion emerges also from the analysis of various contributions to the calculated EFG at Cu, and at Cd substituting at the Cu site, shown in table 1. The EFG is a quantity that efficiently probes the deviation of the electronic density from spherical symmetry. Since both Cu and Cd have a closed-shell (d^{10}) configuration, their ideal electron-density distribution would be spherical and thus the d-electron contribution to the EFG should be zero. The calculated non-zero value for this contribution indicates that the d orbitals of Cu (Cd) stabilize a non-spherical electron distribution, which is a consequence of the crystal field distortion or (and) a hybridization with other orbitals. Both effects are responsible for the large d contribution to the Cu EFG. The Cu d band is positioned near the Fermi level and has large dispersion (figure 2). The Cu d shell extends far enough from the nucleus and thus is not highly localized. Consequently it is susceptible to the action of the crystal field. The Cd d shell, in contrast, is more localized and closer to the nucleus and therefore less influenced by the crystal field. It is mainly the hybridization with Cd s and O p orbitals that makes this shell non-spherical as described in the previous section. The opposite signs of the Cu and Cd d contributions to the EFG (table 1) indicate that the d shells have different non-spherical shapes in these atoms. The anisotropy count Δn_d, for the d shell, is defined as a combination of the subshell occupation numbers inside the atomic sphere: $\Delta n_d = (n_{d_{xy}} + n_{d_{x^2-y^2}}) - (1/2)(n_{d_{xz}} + n_{d_{yz}}) - n_{d_{z^2}}$ and its sign determines the sign of the d contribution to the EFG [14]. The value of Δn_d was found to be +0.195 for Cu, and −0.058 for Cd at the Cu site. The positive sign appears in the first case because the Cu d$_{z^2}$ orbital has the least occupation in comparison with the other Cu d orbitals, while in the case of Cd d$_{z^2}$ has the highest occupation. Indeed, it can be seen from figure 2 that a significant number of Cu d$_{z^2}$ states appear in the conduction band, leaving the occupied valence band with a deficit. In the case of Cd, however, the antibonding orbital appears in the occupied part of the DOS (figure 3), with a considerable content of d$_{z^2}$ states. Thus, a general difference between the Cu and the Cd d-electron clouds in CuAlO$_2$ is that the first is more condensed in the basal plane (only bonding-type orbitals), while in the second case the charge is more stretched towards the oxygens, along the *c*-axis of the crystal. A totally different situation occurs when Cd substitutes at the Al site. In this case the Cd d shell retains its spherical shape and the d contribution to the Cd EFG is close to zero.

According to the present calculations, the electrical properties of the Cd-doped CuAlO$_2$ compound change only when Cd substitutes at the Cu positions. In this case a donor band is introduced inside the forbidden energy gap, near the bottom of the conduction band. Its non-localized nature and the high electron density at the antibonding sites around Cd (figure 4(b)) are typical features of the wavefunction at the bottom of the conduction band in a perfect crystal. This is a characteristic of a shallow band, although the calculated ionization energy (0.122 eV) is too large to support this assumption. The ionization energy is, however, a very subtle quantity and much more refined calculations would be necessary to obtain a reliable

value. The present results, therefore, should be interpreted as an indication that an isolated Cd impurity at the Cu position creates a shallow level in the CuAlO$_2$ spectrum, making the compound an n-type semiconductor. Since impurities with the same $\Delta Z = Z_1 - Z_2$, where Z_1 and Z_2 are the chemical valences of the impurity and the host atom, respectively, generally behave similarly [21], the above conclusions should be valid for Zn and Hg impurities as well.

CuAlO$_2$ is reported to be a p-type semiconductor, due to the presence of natural defects that cause an excess of oxygen [4]. Results of the present calculations indicate that CuAlO$_2$ can also be made an n-type semiconductor by replacing some of the Cu atoms with Cd. Thus, a p–n junction can be constructed from the same material, which would be a highly desirable feature. Following the recently discovery of the CuInO$_2$ compound that has this property [7], we propose that CuAlO$_2$ may be another delafossite that shows bipolarity in electrical conduction. An experimental verification that the Cd substitution of Cu in the CuAlO$_2$ compound does indeed produce an n-type semiconductor would be very important.

5. Conclusions

First-principles FPLAPW band-structure calculations have been performed in order to study the changes in the electronic structure induced by Cd impurity substituting at Cu or Al sites in CuAlO$_2$ delafossite. The calculated EFGs at Cd nuclei are found to be in good agreement with experimental data, especially for Cd at the Cu position, indicating that the present calculations describe the ground state of the system correctly.

The calculations have further shown that the introduction of a Cd impurity causes significant rearrangements of the atoms in CuAlO$_2$, especially those situated near the impurity. The major changes in the electronic structure and the EFG come from the small clusters surrounding the impurity atom. When a Cd substitutes for a Cu, the cluster consists of the Cd, two NN oxygens, and six second-NN copper atoms. When a Cd substitutes for an Al, the cluster contains just Cd and its six NN oxygens.

Through a careful analysis of the electronic structure and EFG values, the characteristic hybridization scheme at Cu sites, proposed earlier [1,2], has been confirmed. This hybridization involves Cu (or Cd substituting for Cu) s and d$_{z^2}$, and NN O p$_z$ orbitals. As a result, the d^{10} shell of these atoms becomes non-spherical, with the d$_{z^2}$ subshell present in several hybrids. The Cu valence band contains only the bonding hybrids $(1/\sqrt{2})(s - d_{z^2})$ at the top and the bonding combination of $(1/\sqrt{2})(s + d_{z^2})$ and O p$_z$ orbitals in the middle. This makes the Cu d-electron cloud compressed within the basal plane due to the small number of d$_{z^2}$ states present. On the other hand, the presence of the antibonding combination of $(1/\sqrt{2})(s + d_{z^2})$ and O p$_z$ orbitals in the occupied part of the Cd spectrum leads to an excess of d$_{z^2}$ states and as a consequence to a larger distortion of the Cd d-electron cloud along the c-axis of the crystal. The antibonding hybrid appears within the CuAlO$_2$ band gap, near the conduction band bottom, with its position controlled by the Cd–O bond distance along the c-axis.

The results from the present calculations strongly indicate that CuAlO$_2$ changes its semiconducting electrical properties when it is doped with Cd atoms substituting at the Cu sites. In this case, n-type semiconductivity is obtained. However, when Cd occupies the Al position, no changes in the electrical properties are observed, i.e. the system does not show the p-type semiconductivity.

Acknowledgments

References

[1] Rogers D B, Shanon R D, Prewitt C T and Gilson J L 1971 *Inorg. Chem.* **10** 723
[2] Orgel L E 1958 *J. Chem. Soc.* 4186
[3] Humberg I and Granqvist C G 1986 *J. Appl. Phys.* **60** R123
[4] Kawazoe H, Yasukawa M, Hyodo H, Kurita M, Yanagi H and Hosono H 1997 *Nature* **389** 939
[5] Otabe T, Ueda K, Kudoh A, Hosono H and Kawazoe H 1998 *Appl. Phys. Lett.* **72** 1036
[6] Duan N, Sleight A W, Jayaraj M K and Tate J 2000 *Appl. Phys. Lett.* **77** 1325
[7] Yanagi H, Hase T, Ibuki S, Ueda K and Hosono H 2001 *Appl. Phys. Lett.* **78** 1583
[8] Buljan A, Alemany P and Ruiz E 1999 *J. Phys. Chem.* B **103** 8060
[9] Yanagi H, Inoue S, Ueda K, Kawazoe H, Hosono H and Hamada N 2000 *J. Appl. Phys.* **88** 4159
[10] Ingram B J, Mason T O, Asahi R, Park K T and Freeman A J 2001 *Phys. Rev.* B **64** 155114
[11] Attili R N, Uhrmacher M, Lieb K P, Ziegeler L, Mekata M and Schwarzmann E 1996 *Phys. Rev.* B **53** 600
[12] Attili R N, Saxena R N, Carbonari A W, Mestnik-Filho J, Uhrmacher M and Lieb K P 1998 *Phys. Rev.* B **58** 2563
[13] Kaufmann E N and Vianden R J 1979 *Rev. Mod. Phys.* **51** 161
[14] Blaha P, Schwarz K and Dederichs P H 1988 *Phys. Rev.* B **37** 2792
[15] Ishiguro T, Kitazawa A, Mizutani N and Kato M 1981 *J. Solid State Chem.* **40** 170
[16] Doumerc J P, Ammor A, Wichainchai A, Pouchard M and Hagenmuller P 1987 *J. Phys. Chem. Solids* **48** 37
[17] Blaha P, Schwarz K and Luitz J 1999 *WIEN97; a Full Potential Linearized Augmented Plane Wave Package for Calculating Crystal Properties* ed K Schwarz (Technical University of Vienna; ISBN 3-9501031-0-4)
This is an updated version of
Blaha P, Schwarz K, Sorantin P and Trickey S B 1990 *Comput. Phys. Commun.* **59** 399
[18] Andersen O K 1975 *Phys. Rev.* B **12** 3060
[19] Perdew J P, Burke S and Ernzerhof M 1996 *Phys. Rev. Lett.* **77** 3865
[20] Benko F A and Koffyberg F P 1984 *J. Phys. Chem. Solids* **45** 57
[21] Bernholc J, Lipari N O, Pantelides S T and Scheffler M 1982 *Phys. Rev.* B **26** 5706